72864

AMPTIAC

AI-AEC-12695
COPY

THERMAL GRADIENT EFFECTS ON STRESS-RUPTURE BEHAVIOR OF THIN-WALLED TUBING

AEC Research and Development Report

DISTRIBUTION STATEMENT A
Approved for Public Release
Distribution Unlimited

ATOMICS INTERNATIONAL

A DIVISION OF NORTH AMERICAN ROCKWELL CORPORATION

Reproduced From
Best Available Copy

20000229 116

LEGAL NOTICE

This report was prepared as an account of Government sponsored work. Neither the United States, nor the Commission, nor any person acting on behalf of the Commission:

A. Makes any warranty or representation, express or implied, with respect to the accuracy, completeness, or usefulness of the information contained in this report, or that the use of any information, apparatus, method, or process disclosed in this report may not infringe privately owned rights; or

B. Assumes any liabilities with respect to the use of, or for damages resulting from the use of information, apparatus, method, or process disclosed in this report.

As used in the above, "person acting on behalf of the Commission" includes any employee or contractor of the Commission, or employee of such contractor, to the extent that such employee or contractor of the Commission, or employee of such contractor prepares, disseminates, or provides access to, any information pursuant to his employment or contract with the Commission, or his employment with such contractor.

Printed in the United States of America
Available from
Clearinghouse for Federal Scientific and Technical Information
National Bureau of Standards, U.S. Department of Commerce
Springfield, Virginia 22151
Price: ~~Printed Copy $3.00; Microfiche $0.65~~

AI-AEC-12695
METALS, CERAMICS,
AND MATERIALS

THERMAL GRADIENT EFFECTS ON STRESS-RUPTURE BEHAVIOR OF THIN-WALLED TUBING

By
JON H. SHIVELY

ATOMICS INTERNATIONAL

A DIVISION OF NORTH AMERICAN ROCKWELL CORPORATION

CONTRACT: AT(04-3)-701
ISSUED: JUNE 25, 1968

DISTRIBUTION

This report has been distributed according to the category "Metals, Ceramics, and Materials," as given in the Standard Distribution for Unclassified Scientific and Technical Reports, TID-4500.

CONTENTS

	Page
Abstract	5
I. Introduction	7
II. Experimental Technique	9
A. Dynamic Sodium Loop	9
B. Test Specimen Description	11
1. High Flux Heater Assembly	11
2. Control Test Assemblies	15
C. Test Procedures and Conditions	15
D. Materials	15
III. Test Results and Analytical Evaluation	17
A. Summary	17
B. Control Tests	17
C. Stress-Rupture Under Steady-State Heating	24
D. Stress-Rupture Under Cyclic Heating	33
1. Results	33
2. Discussion	37
IV. Conclusions	43
References	45

TABLES

1. Systems-Quality Sodium Specification Impurity Limits	9
2. Chemical Composition of Type 304 Stainless Steel	14
3. Biaxial Stress-Rupture With Internal Heating	16
4. Biaxial Stress Rupture Without Internal Heating	18

FIGURES

Page

1. Schematic of Sodium Loop for Test of High Flux Heater Assemblies 10
2. High Flux Heater Assembly 12
3. Imprint of Wire Helix and Associated Polishing on Surface of Control Specimen. 20
4. Fracture Zone at Base of Wire Imprint 22
5. Weld at Interface Between Wire and Cladding 24
6. Heat Zone Temperature Profiles Along Cladding and Under a 10^6 Btu/ft^2-hr Heat Flux 28
7. Predicted Life vs Actual Life of Tubes Under Constant Heating and Pressure 28
8. Longitudinal Strain Profiles of Internally Heated and Pressurized Tubes 29
9. Effect of Stress on Average Strain Rate 30
10. Comparison of Microstructures in Rupture Area 31
11. Predicted Life vs Actual Life for Stress Rupture 36
12. Effect of Thermal Cycling on Stress and Strain Profiles 40

ABSTRACT

The results of stress-rupture tests of internally heated and pressurized thin-walled tubes of Type 304 stainless steel are presented. The tubes were immersed in high-purity sodium at 1200°F and at a flow rate of 20 ft/sec. A heat flux of 10^6 Btu/ft^2-hr passed through the wall. The heat flux was applied in three modes: steady; 6-min on, 6-min off; and 1-min on, 1-min off. The purpose of these tests is to examine the separate and combined effects on creep behavior of stainless steel fuel rod cladding from:

1) Internal NaK pressurization
2) Thermal gradient through the cladding wall
3) Thermal cycling
4) Rate of thermal cycling
5) Mass transfer.

Control tests without internal heating showed that NaK versus helium pressurization and flowing sodium have no effect on the creep behavior. Steady internal heating also has little apparent influence on creep behavior even though evidence of mass transfer was found on the surface. Cyclic heating produced large changes in the microstructures, strain profiles, strain at failure, and the stress-rupture life. Both the reduced life and the attendant strain are explained semi-quantitatively in terms of a ratcheting mechanism using primary creep. These results support the concept that ratcheting of the cladding due to reactor load variations is a distinct possibility and that this must be considered in designing fuel elements for long life and high power density operation.

I. INTRODUCTION

The goals of the experimental effort described in this report are to study the combined and separate effects of the non-nuclear aspects of liquid metal cooled fast reactor service conditions on potential fuel cladding material. The work is aimed at providing data under simulated reactor service conditions without the complicating effects of radiation. These conditions are:

1) Biaxial stresses due to fission gas pressure and fuel swelling
2) Mass transfer due to high temperature flowing sodium
3) Thermal stresses due to high heat fluxes
4) Thermal cycling due to variations in reactor power loading.

In addition to irradiation effects, interaction of these service conditions with the mechanical properties of cladding material limit the service life.

Much of the behavior associated with the non-nuclear aspects of fast reactor environmental conditions is not well understood. Because of the critical nature of fuel cladding, from both an economic and safety viewpoint, designers of core assemblies will require more data and information about the environmental effects on cladding mechanical behavior. The purpose of this testing program is to contribute to a better understanding of the environmental effects, as well as to provide design information for application of cladding materials.

The technical approach is to compare the combined environmental effects with suitable control properties in static and dynamic sodium. This approach is both convenient and fruitful because of the extensive biaxial stress rupture data obtained in static sodium.[1] Using those data for control, it is possible to differentiate the separate non-nuclear aspects of the reactor environment. This involves the effects of NaK pressurization versus helium pressurization, flowing sodium versus static sodium, thermal stresses imposed by heat flux through cladding, and cyclic thermal stresses superimposed on steady state loading on the rupture life of cladding.

The results from this work are expected to provide insight into the relative magnitude of the separate and combined effects of the non-nuclear part of

the reactor environment. Of particular interest is the effect of thermal cycling and the mechanism operating under this condition. For convenience, the time of testing is less than desired in actual application. Nevertheless, if a set of equations which adequately describe the phenomena could be obtained, accurate extrapolation of the data to design lifetimes may be carried out. The results of the tests were expected to be partly diagnostic, insofar as this kind of test had not been performed previously. Therefore, the results were intended to serve a dual purpose of identification of the environmental effects and their interactions, as well as semiquantitative determination of their magnitude in support of establishing design criteria.

II. EXPERIMENTAL TECHNIQUE

A. DYNAMIC SODIUM LOOP

A two-inch dynamic sodium loop was used to test and evaluate the effects of environmental factors on the mechanical properties of fuel cladding. This facility enables cladding to be exposed to isothermal flowing sodium at temperatures up to 1300°F and velocities up to 20 ft/sec.

The general layout of the loop is shown in Figure 1. The loop has several features which bear a direct relation to the stress-rupture tests performed on cladding. These features permit the total environment experienced by the cladding to be specified and held constant.

The sodium chemistry is carefully controlled and monitored by sodium plugging runs and by periodic sodium sampling and cold trapping. As a result, the sodium chemistry has remained essentially constant from the beginning of this program. Analyses of the "systems quality" sodium used in the two-inch loop consistently fell at or below the specified impurity limits shown in Table 1. The specifications for the systems quality sodium used in this loop are described elsewhere.[2] The analysis displayed in Table 1 is important since corrosion and mass transfer are quite dependent on the concentration of these particular species.

TABLE 1

SYSTEMS-QUALITY SODIUM SPECIFICATION IMPURITY LIMITS

From Specification ST0170NB0047

Element	Impurity (ppm)
C	12
Cr	5
Fe	20
Ni	10
O	10

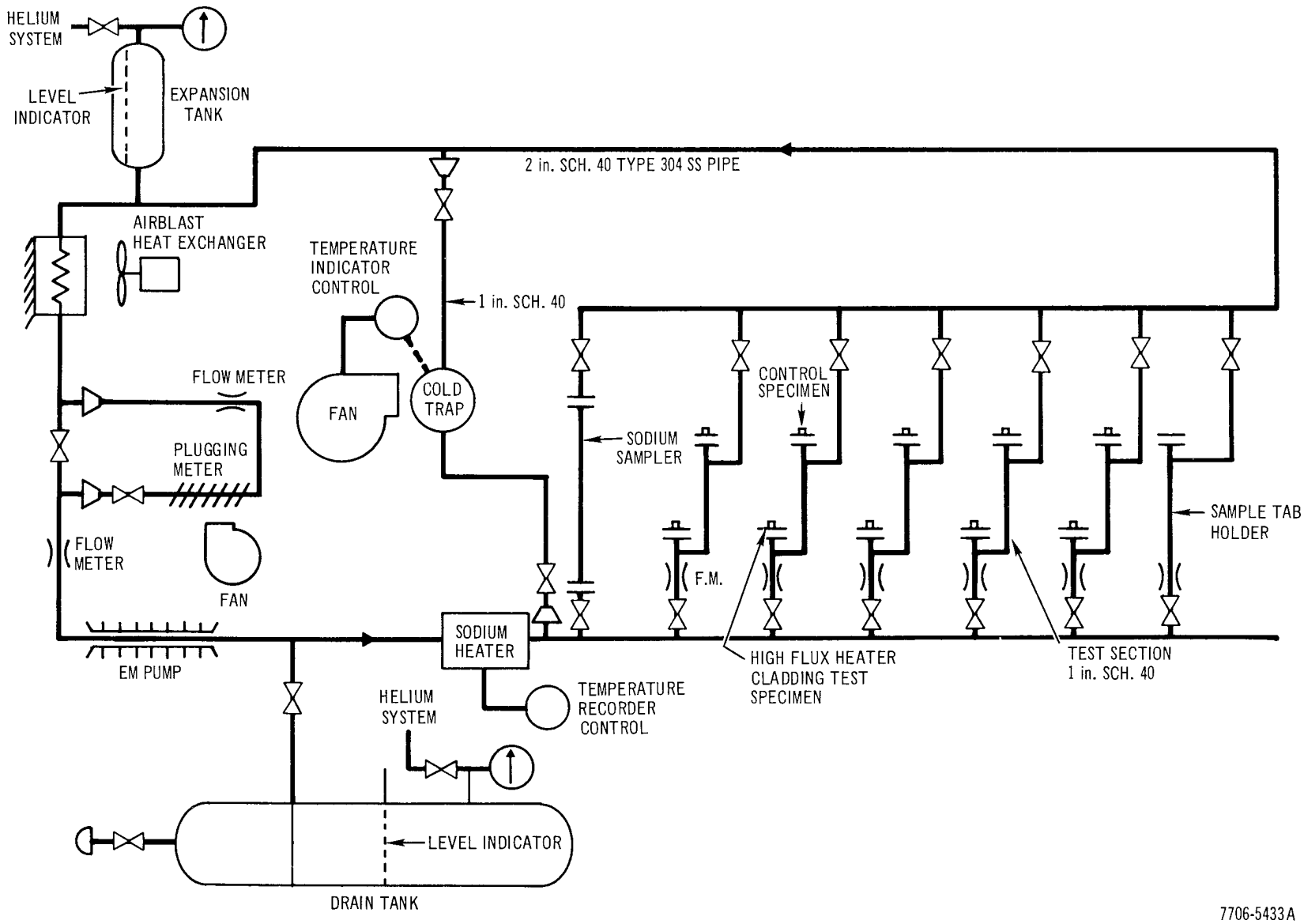

Figure 1. Schematic of Sodium Loop for Test of High Flux Heater Assemblies

The temperature of the loop is held constant in the test sections of the loop, although radiant heat losses through the walls do cause a 20° temperature gradient around the loop. The temperature at the inlet and outlet to each test station can be continuously monitored and generally does not vary more than 3°F during the tests. The calibration of these thermocouples is maintained. As a result of the operation of the high heat flux assemblies with or without cladding, the temperature at the outlet in a given test section is raised about 25°F; this is particularly important when two tests are conducted in series since outlet becomes the inlet for the next test, raising the sodium temperature in the next test section. For parallel test sections, no differences in temperature are encountered since the inlet temperature to each section is the same.

The flow rate of sodium is preset in each test section before the test on cladding is started, and it is followed during the course of testing. Flow rates are measured using the magnetic technique. The magnets are precalibrated and are checked periodically.

Another feature of the isothermal sodium loop is the ability to cold trap the sodium prior to testing. This permits impurities to be removed and has been used successfully in other loops to maintain and improve the purity of the sodium. The cold trapping procedures have been held constant. This accounts for the nearly constant chemistry of the sodium in this loop and an essentially constant sodium plugging temperature of 210°F.

B. TEST SPECIMEN DESCRIPTION

1. High Flux Heater Assembly

The ability to internally heat and pressurize the tube samples represents a new and significant step toward a better understanding of the behavior of cladding in a nuclear environment. This simulates the effect of heat transfer from the fuel to the coolant and the effect of gas pressure and fuel swelling on the cladding. To achieve this ability, it was necessary to design and develop a high heat flux (10^6 Btu/ft^2-hr) resistance heater to be inserted inside the cladding in such a way that the cladding could be internally pressurized. In addition, the heater must operate for a sufficiently long time to obtain meaningful creep-rupture results. The current design of the high flux heater assembly

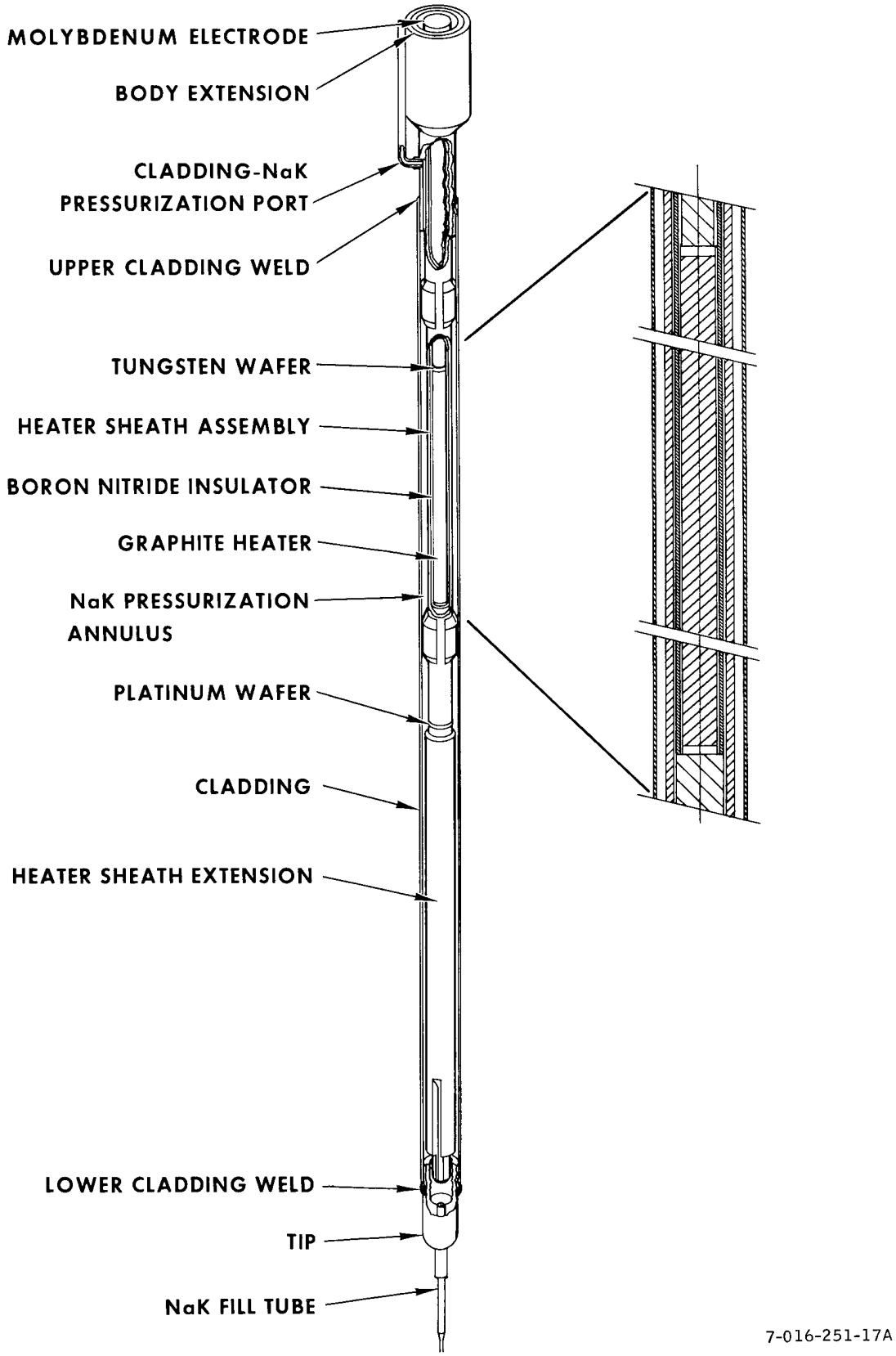

Figure 2. High Flux Heater Assembly

with cladding is shown schematically in Figure 2. The developmental work and the design features of the heater assembly are described elsewhere.[3]

It is necessary to describe certain features of the heater assembly to give a sufficient background to the observations connected with these tests. The heater consists of a two-inch graphite cylinder inserted into a hollow stainless steel sheath but insulated from the sheath by a boron nitride sleeve. The graphite is separated from the bottom of the sheath with a platinum diffusion barrier. A tungsten wafer serves the same purpose at the top between the graphite and the molybdenum electrode used to supply electrical power to the graphite barrier. Electrical current flows through the molybdenum, to the graphite, to the heater sheath. The circuit is completed through the sodium back to electrical ground.

The outside of the heater sheath contains two centering lobes which ensure that the heat zone is concentrically located inside the cladding. The cladding is welded to the top and the bottom of the sheath and high purity NaK is loaded through a tube in the bottom. The NaK is used to provide a heat transfer medium between the sheath and the cladding and to enable mechanical stresses to be exerted on the cladding. This is accomplished by a bellows pressurization system. Very simply, the diaphragm of the bellows transfers pressure from high purity helium to the NaK when the tube at the bottom of the sheath is closed. The diaphragm can move sufficiently to compensate thermal expansion of the cladding, and subsequent creep strain, during the test without a decrease in pressure.

The cladding on the heater assembly is surrounded with a test assembly (shroud). The purpose of this shroud is to provide a convenient means of locating the heater assembly in the sodium test loop as well as to provide a channel for turbulent flow. A wire helix on the inside surface of the shroud promotes turbulence and hydraulically centers the assembly in the channel. The lower end of the shroud assembly fits into a locating slot in the dynamic sodium loop test section which is designed to prevent by-pass flow.

Electrical connections and helium pressurization are provided as part of the sodium loop operations. An added feature of this facility is that the electrical power to the heaters can be cycled on and off at different frequencies. This enables the effects of thermal cycling on the creep-rupture properties to be studied.

TABLE 2

CHEMICAL COMPOSITION OF TYPE 304 STAINLESS STEEL (Heat No. 20013)

Element	Weight %
Cr	18.66
Ni	9.30
Mn	1.50
Si	0.30
Mo	0.22
Cu	0.20
C	0.06
P	0.03
S	0.03
Co	0.01
B	0.0005
N	0.075
Fe	Balance

2. Control Test Assemblies

The control test assemblies are identical to the heater assemblies, except that there is no heating element. Both the geometry and the hydraulic aspects are identical. Specifically, the control assemblies use NaK to pressurize the cladding.

C. TEST PROCEDURES AND CONDITIONS

The heater assemblies are sealed into the dynamic sodium loop and the loop is evacuated to remove most of the oxygen and to assist in filling the loop with sodium. In some cases, control test assemblies were inserted downstream from heater assemblies. The sodium is circulated at a low temperature while the sodium is cold-trapped. Once the plugging run gives a positive indication that the loop sodium is sufficiently cold-trapped, the bulk sodium temperature is brought to 1200°F and the flow at 20 ft/sec. To start the test, the electrical power to the heater is set to give a 10^6 Btu/ft^2-hr heat flux at the cladding surface, and the pressure is applied at a prescribed level. Both the pressure and the electrical power are continuously monitored during the test. The electrical circuit is also equipped with a transient detector which prevents heater failures due to minor excursions in electrical power during the test. This device is particularly important when the heaters are operated in cyclic mode. The test is terminated when the pressure level drops below a certain value, indicating a rupture of the cladding. This constitutes the time for failure. A pressure switch automatically cuts off the power to the heater. Once the test is complete, the sodium flow is reduced so as to reduce the temperature in the test section until the assembly can be removed from the loop.

D. MATERIALS

The material used for this study is Type 304 austenitic stainless steel seamless tubing of nominal 0.295-in. OD by 0.010-in. wall. The chemical composition of this characterized heat is displayed in Table 2. The material was used in the as-received condition which contains from 10 to 15% cold work. The grain size was ASTM 8.[4] This particular heat of stainless steel is thoroughly characterized from the ladle to the end product. The processing history includes hot finished extrusion and then reduction to a size of 7/8-in. OD by 0.083-in. nominal wall. A normal cycle of degreasing, annealing, pickling, and cold-drawing was performed to obtain the finished form.

TABLE 3

BIAXIAL STRESS-RUPTURE WITH INTERNAL HEATING

Specimen No.	Heat Flux (Btu/ft^2-hr)	Heat Flux Condition	Rupture Time (hr)	Mechanical Hoop Stress (psi)	Calculated Thermal Stress (psi)	Peak Strain (%)	Peak Strain Rate† (in./in./hr)	Actual Life / Predicted Life§
30	1×10^6	Steady	177	21,000	8,300	2.2	1.2×10^{-4}	0.9
36	1×10^6	Steady	558	16,000	8,300	2.8	4.5×10^{-5}	1.1
34	1.5×10^6	12-min cycle	5*	21,000	12,400	3.6	-	-
38	1×10^6	12-min cycle	198*	16,000	8,300	1.0	1.1×10^{-4}	-
32	1×10^6	12-min cycle	227	21,000	8,300	3.6	3.2×10^{-4}	0.57
40	1×10^6	12-min cycle	173	21,000	8,300	3.6	4.2×10^{-4}	0.43
42	1×10^6	2-min cycle	134	21,000	8,300	3.6	5.4×10^{-4}	0.33
44	1×10^6	2-min cycle	163	21,000	8,300	3.6	4.4×10^{-4}	0.41
46	1×10^6	12-min cycle	398	17,700	8,300	3.6	1.8×10^{-4}	0.55
48	1×10^6	12-min cycle	419	17,700	8,300	3.6	1.8×10^{-4}	0.56

*Heater failed prior to cladding

† Based on the time the heat flux is on

§Prediction is based on isothermal data obtained in static sodium

III. TEST RESULTS AND ANALYTICAL EVALUATION

A. SUMMARY

Ten tests have been conducted with internally pressurized and heated cladding in flowing sodium at 1200°F and at a velocity of 20 ft/sec. The results of these tests are presented in Table 3. The heaters were operated in a steady-state condition and two cyclic conditions, a 12- min cycle and a 2-min cycle.

Four tests with control assemblies have been performed with internal pressurization only. The results of these tests are displayed in Table 4. It should be noted that these tests were conducted in series, and downstream from the heater assembly tests. As a result, the sodium temperature was raised for part of the test by the local heating of the sodium. After the tests of the heater assemblies were complete, the sodium was no longer heated. Thus, the entire test was not performed at the same temperature. The temperatures reported for the control tests in Table 4 reflect the variances by averaging for the time spent at each temperature.

B. CONTROL TESTS

To establish the validity of the results obtained from specimens which are both heated and pressurized internally, it is necessary to employ control tests. The purpose of the control experiments is to determine the effect, if any, of NaK pressurization on the stress-rupture and creep behavior of cladding. This need arises because NaK may reduce the life of cladding by action at the inside surface of the cladding specimen. For example, the removal of the oxide surface layer may reduce the surface barrier to dislocations, or NaK may penetrate the metal along grain boundaries and reduce the load-carrying capacity of the metal. In either case, these experiments will serve to ascertain the influence of NaK on the stress-rupture behavior.

Biaxial stress-rupture tests have been conducted on tubes of Type 304 stainless steel from the same heat and with the same fabrication history. These tests were internally pressurized with helium and were exposed to either static sodium or helium gas. This work provides a convenient base line to which the tests in dynamic sodium can be compared.[1]

TABLE 4

BIAXIAL STRESS RUPTURE WITHOUT INTERNAL HEATING

Specimen No.	Heat Flux (Btu/ft^2-hr)	Heating Condition	Rupture Time (hr)	Mechanical Hoop Strain (psi)	Maximum Hoop Strain at Failure	Average Temperature (°F)	Actual Life / Predicted Life
31	0	No Heat Flux	750	26,000	2	1210	1.0
33	0	No Heat Flux	931	19,000	0	1245	0.88
35	0	No Heat Flux	351	26,000	1	1245	0.9
37	0	No Heat Flux	479	26,000	1	1235	1.1

Stress-rupture data on control specimens in dynamic sodium were compared to the stress-rupture data obtained in static sodium. The data for control specimens in flowing sodium superimpose on the stress-rupture data obtained in static sodium within the uncertainty in temperature. This means that NaK pressurization and dynamic sodium did not substantially alter the biaxial stress-rupture life of cladding.

The absence of a NaK pressurization effect is not unexpected when consideration is given to recent work in static sodium and helium.[1] In the case of both Type 304 and Type 316 stainless steels, the behavior in helium and in sodium were identical within normal experimental scatter. Thus, the total results of tests in helium, static sodium, and dynamic sodium support the concept that neither NaK pressurization nor the sodium environment affects the life of cladding under isothermal test conditions.

Microstructural observations give added support to the lack of an effect of NaK pressurization as well as the flowing sodium environment. The salient features of the microstructures of control specimens are identical to those observed after testing in static sodium. The presence of voids at grain boundaries, intergranular failures, carbide precipitation phenomena, and the absence of sigma phase are all similar. Thus, the mechanisms leading to failure do not appear to be sensitive to the external environment. Rather, these are related to load, temperature, and geometry. No evidence of intergranular penetration by either NaK or the sodium was found at either surface. The results of the tests in dynamic sodium and in static sodium strongly suggest that these environments do not inherently reduce the stress-rupture life of cladding.

One important observation from the microstructural observations is that all of the control specimens tested in flowing sodium exhibited a thin surface layer, probably ferrite. The thickness of the layer varied from specimen to specimen, depending on the temperature and the duration of exposure to sodium, and ranged up to 0.3 mil. Magnetic measurements confirmed the presence of ferrite on three of the specimens.

The presence of a ferrite layer on the control specimens (not internally heated) can be explained. In order for mass transfer effects (corrosion and ferrite layer formation) to occur, two conditions must be fulfilled:[5]

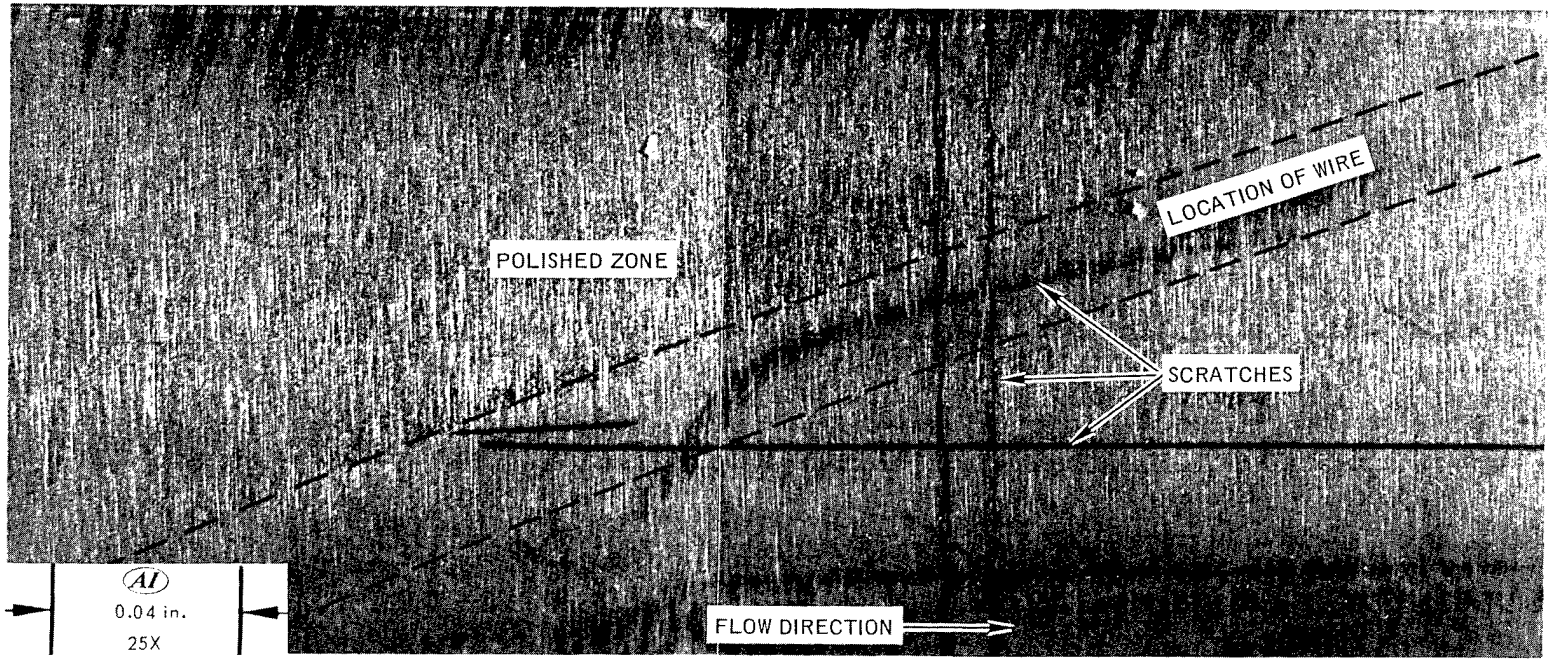

UNETCHED

8038-2-2-3

Figure 3. Imprint of Wire Helix and Associated Polishing on Surface of Control Specimen

1) The concentration of the transported species must be locally undersaturated in the bulk sodium.

2) The kinetics of transport must be fast enough to permit transfer to occur in a reasonable amount of time.

For the formation of ferrite layers on austenitic stainless steels, these criteria mean that the sodium is unsaturated with respect to nickel and that the rate of diffusion of nickel is sufficiently fast to enable the ferrite layer to grow. The kinetic criterion is fulfilled because the sodium velocity was 20 ft/sec and the temperature was above 1200°F. The undersaturation of the bulk sodium with respect to nickel occurred because the temperature of the sodium was raised. This local increase in temperature in the control test leg was first created by the presence of a heater upstream from the control specimen. Later, after the heater was removed from the loop, the bulk sodium temperature was raised 25°F to simulate the temperature condition created by an upstream heater. Thus, the control specimens spent the majority of their lives exposed to sodium at a slightly higher temperature. Apparently this temperature increase was sufficient to increase the solubility of the sodium for nickel and to permit mass transfer to occur.

An important question relevant to this work is the influence of a ferrite layer and associated surface removal on the mechanical properties of cladding materials at elevated temperatures. While this question is yet unanswered for long-term tests, the ferrite layer does not appear to adversely affect the stress-rupture behavior for times less than 1000 hours.

In the case of the control specimens, the cladding interacted with the wire helix on the inside shroud subassembly which surrounds the cladding. A wire helix of Type 304 stainless steel on the inside surface of the shroud acts to promote turbulence and hydraulic centering vital to the stress-rupture and mass-transfer behavior of the internally heated specimens. However, the shroud played an active role in the behavior of the control specimens without internal heating, as evidenced by the presence of a polished zone on the surface of the cladding adjacent to the wire of the helix (corrosion) and in the presence of a ferrite layer on the surface of the control specimens (selective attack). As shown in Figure 3, a polished zone was observed on certain areas of the surface

of the control specimens. While corrosion and selective attack were observed, no effect on the mechanical properties was observed. Cracking was not associated with either the polishing or with the ferrite layers.

The wire helix interacted with the cladding in another way which has important implications in the design of fuel assemblies. For the control specimens only, the strain was not limited to the upper regions above the helix but was uniformly distributed along the length. As a result of uniform strain in the control tests, the cladding impinged on the wire helix forcing it tightly against the inside surface of the shroud. This resulted in an imprint of the wire on Assembly No. 31 of the control test. It should be noted that this specimen showed the greatest diametral strain, 2%.

Perhaps more significant to fast reactor technology is that the failure occurred at the bottom of a small section of the deformed region associated with the wire helix. This failure was sectioned, and a photomicrograph of the failure is shown in Figure 4. The technical implication of this observation to the fast reactor wire wrap concept for fuel cladding is obvious. While the conditions

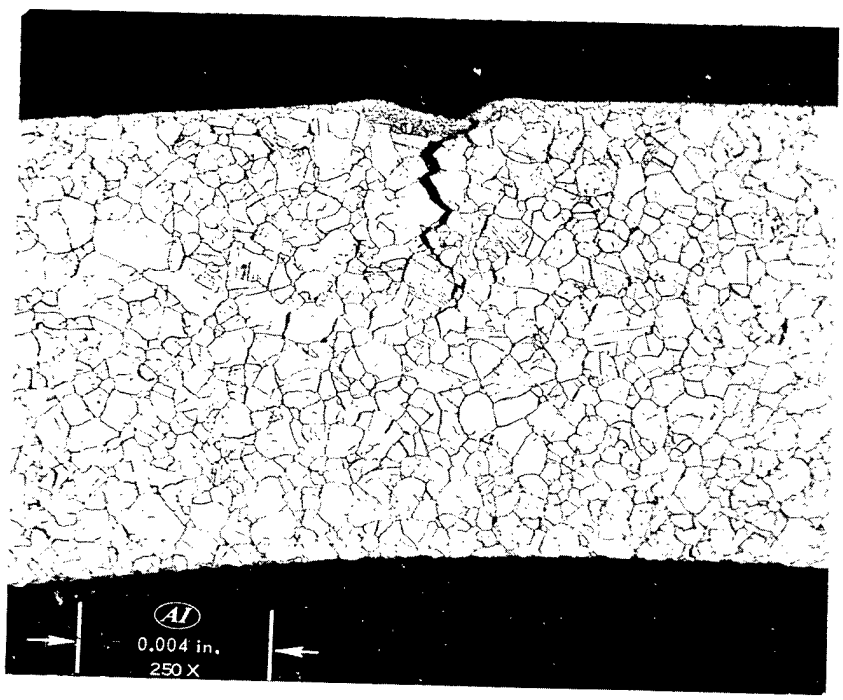

RIETH'S ETCH

8038-15-1

Figure 4. Fracture Zone at Base of Wire Imprint

associated with the shroud assembly cladding interaction by no means duplicate the conditions associated with those anticipated for a wire wrap, it is clear that localized deformation zones on the surface of cladding can play a role in the formation of cracks. The formation of stress concentration centers on the cladding surface may reduce the life under stress. However, for the short term control test, the rupture life did not appear to be significantly affected by the imprint. It is perhaps dangerous and premature to argue that the long-term life of a specimen in which this phenomenon occurs would not be adversely influenced.

Other investigators have observed premature failures due to wire wrap.[6] In this case, the wire separated inner and outer containment vessels from each other in a fuel assembly. Premature failure resulted when the wire interacted with the two vessels. This observation, coupled with the one reported here, suggests the need for additional information concerning the potential problems of employing wire-wrapped cladding to promote mixing of the coolant.

In addition to the wire imprint interaction described above, another interaction between the wire helix and the cladding was observed. This interaction was a pressure bonding of the cladding to the wire at one point to the test specimen of control test in Assembly No. 33. No other welds were found. The bond shown in Figure 5 extended 1 mil into the cladding. Flaw detection indicated two possible sites for failure, one at a conventional site and one at the weld region. No cracks were evident in the microstructure at either location. This inability to locate the fracture is not uncommon. A similar difficulty in finding cracks has sometimes occurred for specimens tested in static sodium. Basically, it is believed that failures in these cases are best described as pin holes rather than tube bursts. In any case, it is entirely possible that incipient cracking took place in the region surrounding the weld zone.

This effect of pressure bonding of stainless steel in liquid sodium type environments is not new.[7] Of all the control specimens tested thus far, this specimen with the weld interaction showed slightly less correlation with an interpolation of the data obtained in static sodium. However, all of the control specimens agreed with the behavior in static sodium within limits of the expected experimental scatter and the limits of the precision in the interpolation of static sodium data.

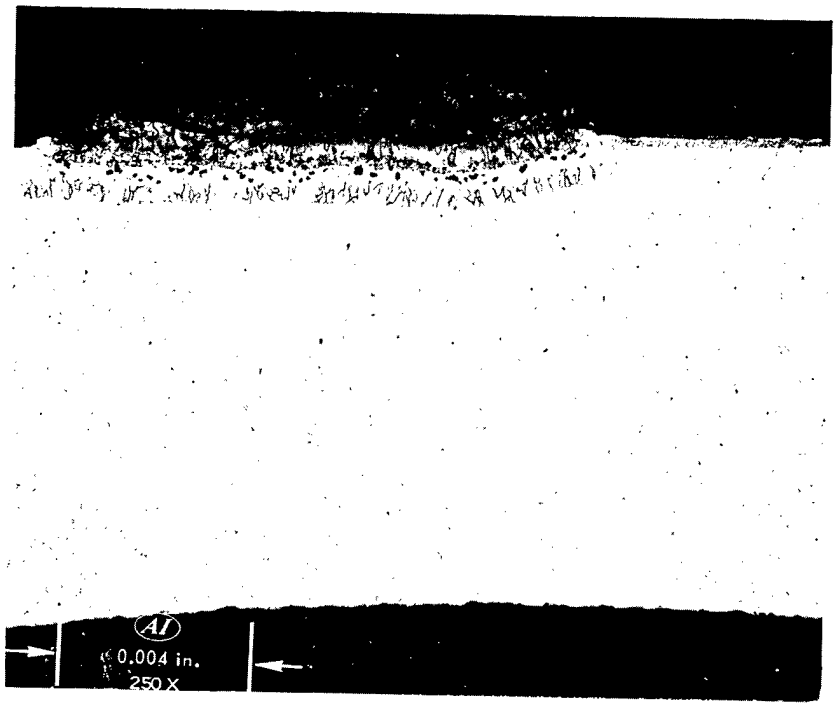

VILELLA'S ETCH

8038-12-4

Figure 5. Weld at Interface Between Wire and Cladding

In summary, the effects of NaK pressurization or corrosion on the stress-rupture behavior of internally pressurized tubes in a flowing sodium environment are too small to be detected in the time scale of these tests. Examples of interactions which are estimated to have no effect on the short-term properties remain possible problem areas for long-term tests. While these aspects are of interest, the control tests completely verified the use of NaK as a means of internally pressurizing cladding during tests even when cladding is under internal heating.

C. STRESS-RUPTURE UNDER STEADY-STATE HEATING

The purpose of tests of both internally pressurized and heated specimens in dynamic sodium is to simulate conditions anticipated in fast reactors for fuel cladding. As a direct result of internal heating, thermal stresses are generated, interstitials migrate up the temperature gradient, and the conditions favoring mass transfer are formed. It is vital to the designer of fuel pins to be able to assess the magnitude of these effects both separately and in concert.

For stress-rupture under internal heating and pressure, it is important to determine the stresses present in the metal. This is important so that meaningful comparisons between these tests and those conducted in static sodium can be drawn. The mechanical stresses were calculated using the thin wall cylinder formula for internal pressurization.

$$\sigma_h = Pr/t \qquad \ldots(1)$$

where

σ_h = hoop stress

P = internal pressure

r = radius of the inside

t = thickness

and the axial stress is one-half the hoop stress.

In the absence of plastic deformation, the thermal stresses at the outside surface of the cladding in both the longitudinal and transverse directions are given by

$$\sigma_t = \frac{E\alpha\Delta T}{2(1 - \upsilon)} \qquad \ldots(2)$$

where

σ_t = thermal stress,

E = Young's modulus,

α = coefficient of linear expansion,

ΔT = wall temperature difference, and

υ = Poisson's ratio.

For the present tests with a heat flux of 10^6 Btu/ft^2-hr and thermal gradient of 50°F, the corresponding thermal stress is 8300 psi at the peak temperature position. It should be noted that the thermal stress is tensile at the outside surface and compressive at the inside surface of the tube.

Before a comparison can be made between the results of the tests in flowing sodium with internally heated and pressurized tubes and the results in static sodium with internally pressurized tubes, several factors must be considered:

1) Stress relaxation by creep

2) Temperature distribution effects

3) Uncertainty in the temperatures.

These factors are important because creep is an exponential function of temperature and stress.

For creep under combined mechanical and thermal stresses, it is to be expected that, due to stress relaxation, the thermal stresses will disappear. The amount of stress relaxation at the outer fiber due to secondary creep can be estimated from the creep equation. However, this estimate is too low because the initial loading from internal pressure, and from the heat flux through the wall, will produce a certain amount of primary creep. Since the strain associated with the creation of thermal stresses is small, $\epsilon_t = 10^{-5}$, almost all of the thermal stress is removed by deformation on loading. This gives rise to nonuniform straining across the wall of the tube. It is this strain gradient that plays a crucial role in the behavior of the thermally cycled specimens. This point will be discussed later. For the steady-state heating, the important fact is that the thermal stress is relaxed from primary creep and then secondary creep occurs under the combined action of the stress and temperature.

The behavior of the cladding is complicated by the presence of the thermal gradient through the wall because the secondary creep rate is an exponential function of temperature. Thus, if the outer fibers in the tube wall are stressed the same as the inner fibers (thermal stress is completely relaxed), the hotter inner fibers would tend to deform faster than the cooler outer fibers. From a standpoint of plasticity theory, this condition cannot prevail without producing internal stresses which counteract the non-uniform deformation or without violating the material compatibility relations. However, if the thermal stress relaxed only enough to cause the cooler outer layers to creep at a rate equal to the hotter inner layers, the resulting thermal and stress gradients would be self-compensating. This action results in a uniform strain rate across the tube wall.

For the case where the temperature difference between the two walls of the tube is small (50 °F), the two gradients intersect at the midwall position. This means that creep of the steady-heated specimens can be best described by the conditions at the midwall position.

The conclusion that the secondary creep rate at the center of the wall is the overall creep rate for the tubes, once the initial compensating aspects have occurred, enables the tests in static sodium to be compared directly to the tests of steadily heated specimens in flowing sodium. Before such a direct comparison can be made, some mention of the temperature distribution associated with the tests under steady-state heating should be made. The distribution of temperature through and along the wall is displayed in Figure 6. Clearly, creep and the associated failure will occur at the highest temperature and stress point; therefore, if the tests with internal heating are to be directly compared to the tests in static sodium, they should be compared at the temperature and stress at the midwall in the peak region.

The comparison between the tests in static sodium and the tests in flowing sodium with internal heating is displayed in Figure 7. The temperature band represents the uncertainty in the expected behavior based on static sodium data and was drawn by interpolating the static sodium data for the limits of uncertainty in the peak midwall temperature of the internally heated tubes. On the basis of this interpolation, it appears that the behavior of the tubes under internal heating and pressure can be predicted from isothermal stress-rupture data for the peak temperature conditions. Thus, while the presence of a high heat flux complicates the interpretation of the behavior, in the last analysis creep is, under a steady state thermal gradient, primarily a function of stress and temperature. If these two factors are known with some certainty, the behavior can be directly predicted from isothermal test data.

The strain profiles of tube tests with internal heating follow the temperature profile along the wall of the tube, as illustrated in Figure 8. The failure occurred in the peak strain position, which is also the peak temperature position. This observation conforms with what is to be expected for creep deformation under a steady state heating condition in flowing sodium. Comparing static and flowing sodium results, several reasons for a lower average strain rate or

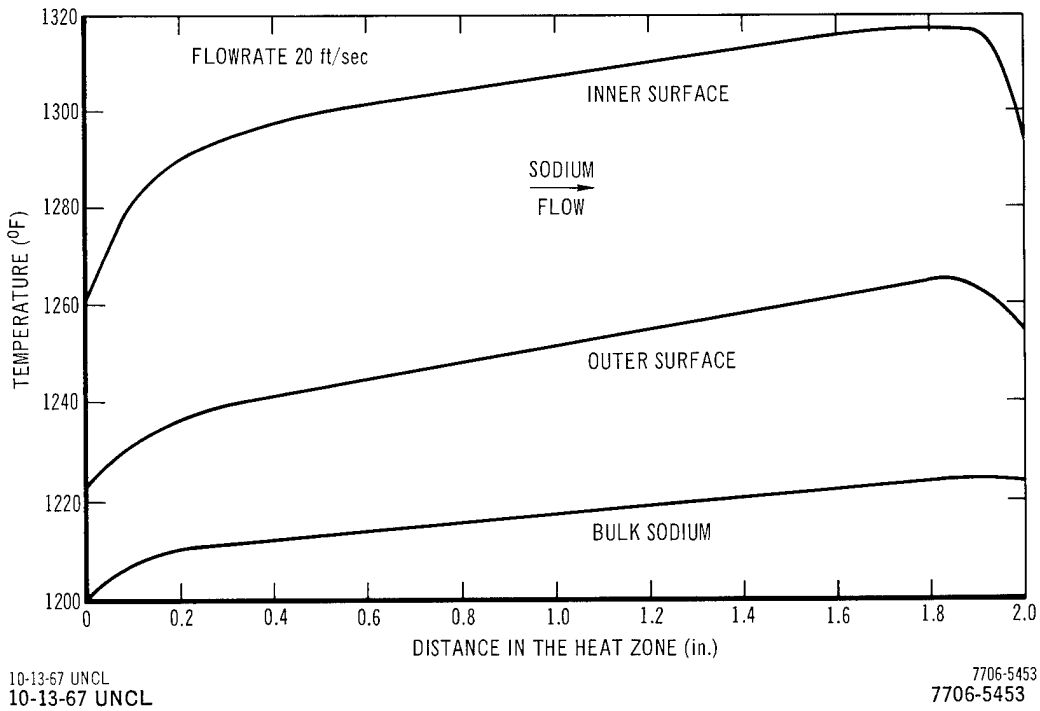

Figure 6. Heat Zone Temperature Profiles Along Cladding and Under a 10^6 Btu/ft^2-hr Heat Flux

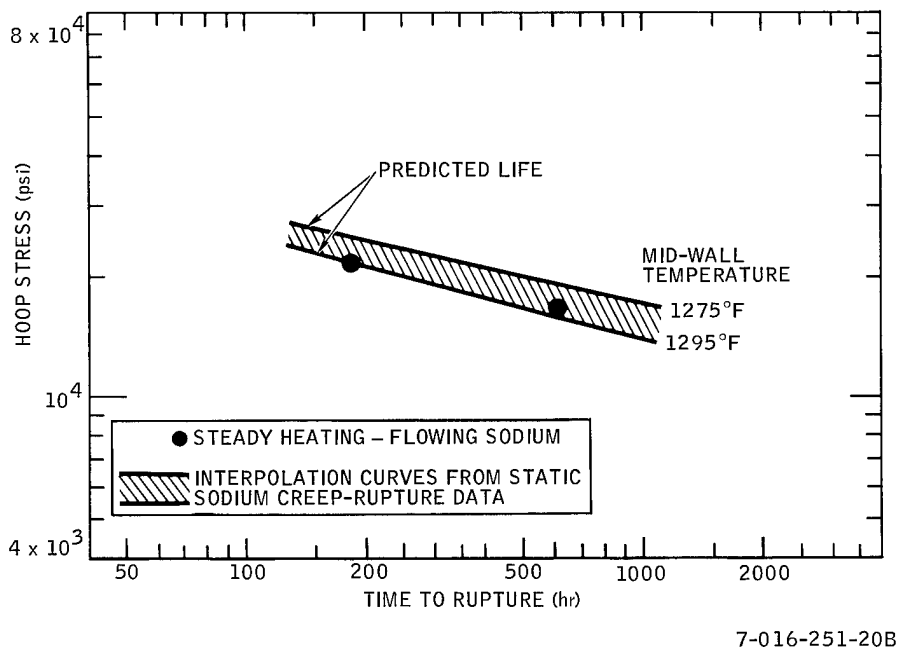

Figure 7. Predicted Life vs Actual Life of Tubes Under Constant Heating and Pressure

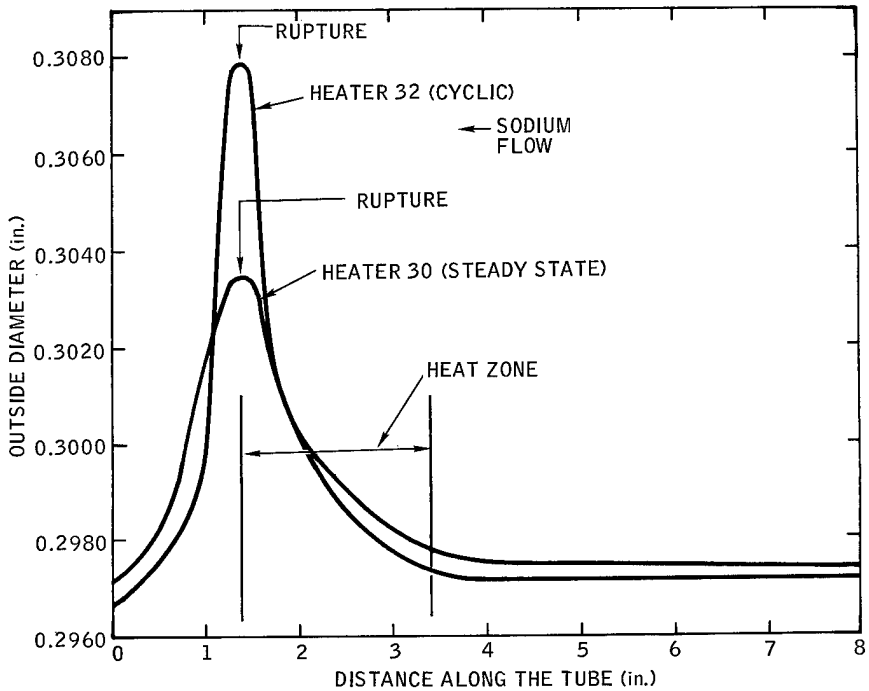

7-016-251-22-1A

Figure 8. Longitudinal Strain Profiles of Internally Heated and Pressurized Tubes

lower strain to failure under internal heating can be advanced. The observed strain distribution implies that deformation takes place over a smaller region due to the temperature and stress variation along the wall. Consequently, the cooler (and stronger) metal offers constraint to plastic flow to the hotter (and weaker) metal because of the compatibility condition of plasticity theory. Such action may effectively strengthen the weaker metal but render it less ductile. This does not necessarily mean that the life under stress is reduced. A similar circumstance is found in the notch effect in stress-rupture tests where in some cases the life is actually extended. It is too early to judge whether such effects are present in the present tests.

It is instructive to compare the average strain rate (strain at failure divided by the time to failure) for the hoop direction in both the static and dynamic sodium tests. As before, it is possible to make a comparison by drawing the strain rate-stress curves for the uncertainty in temperatures found at the peak midwall position for the internally heated tubes. Using the stress and

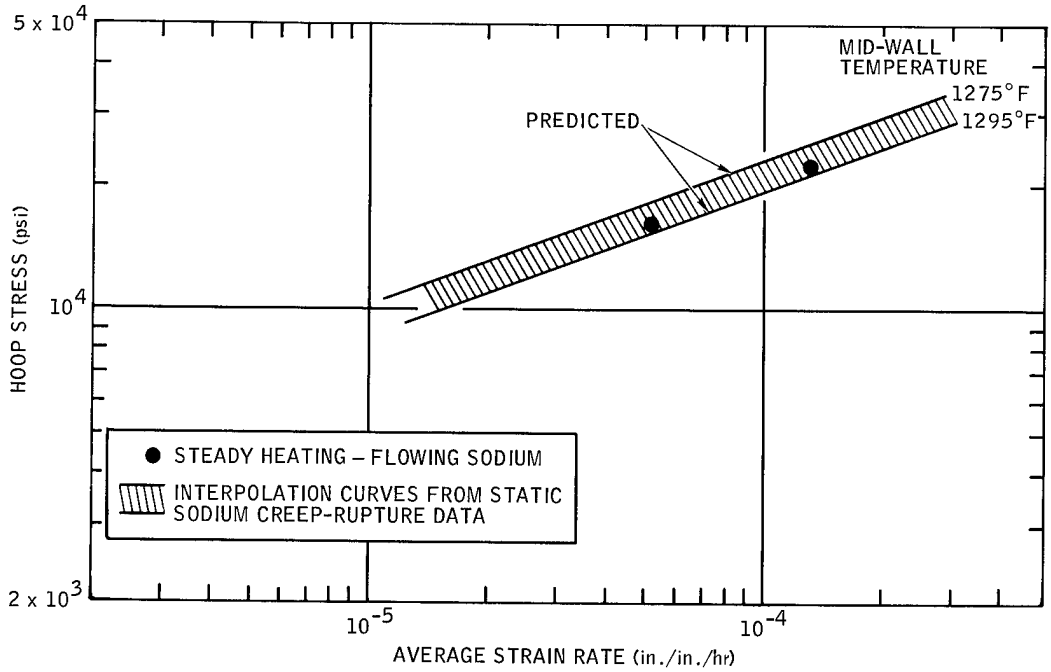

8-MA15-084-1

Figure 9. Effect of Stress on Average Strain Rate

temperature range at the midwall point, the present tests fall within the band, as shown in Figure 9. The close agreement between the tests in dynamic sodium with internal heating and pressure and the predicted behavior derived from static sodium data strongly supports the concept that the creep behavior, and probably failure, are governed by the stress and temperature at the peak temperature position and at the midwall location.

The microstructures of specimens tested with internal pressure in static sodium and the specimens tested with internal heating and pressure in dynamic sodium are essentially the same. The microstructures of the internally heated specimens are shown in Figure 10. In summary, the microstructures exhibited:

1) Intergranular failure

2) Extensive void formation throughout the wall

3) Little or no sigma phase

4) Carbide precipitate at the grain boundaries.

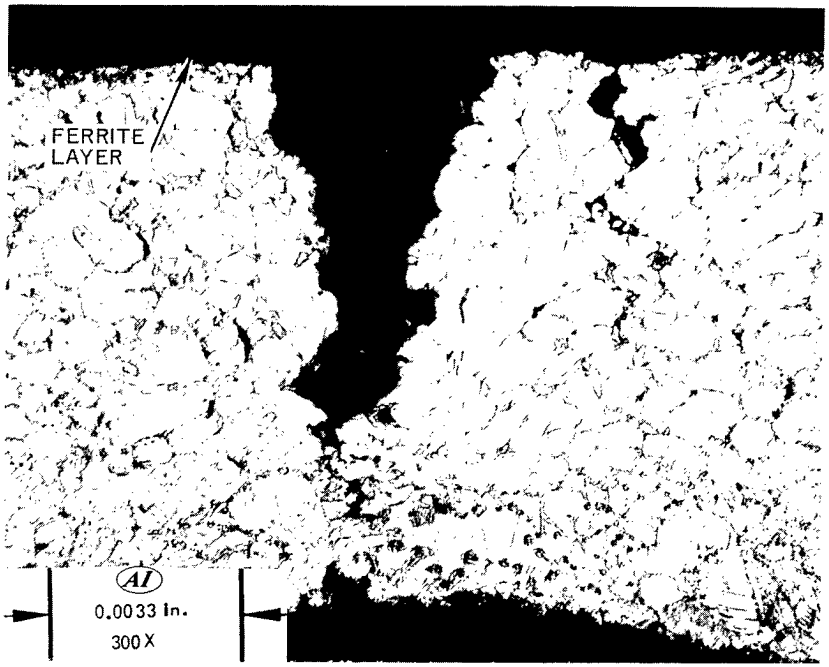

Etchant: Marble's Solution 7968-12B-16

a. Cyclic

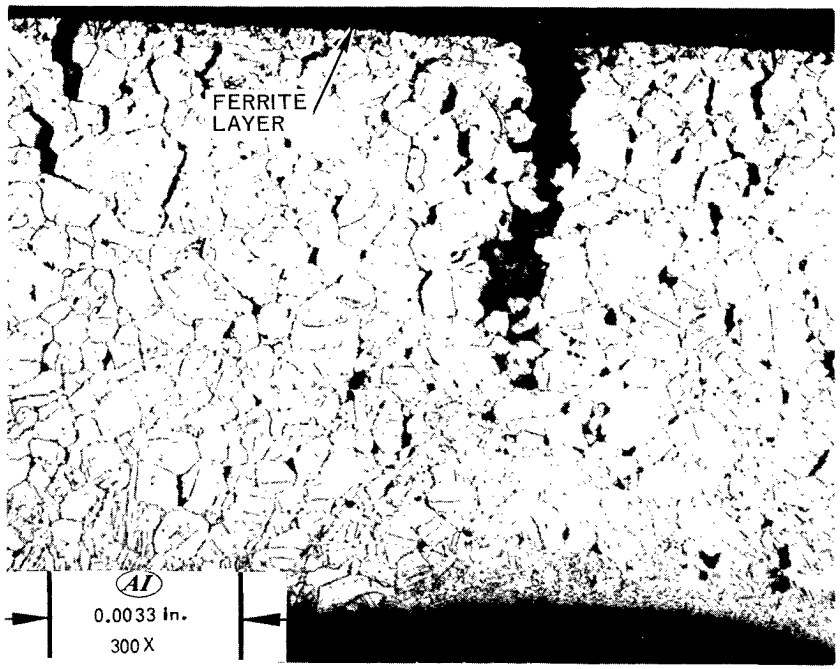

Etchant: Marble's Solution 7968-6B-7

b. Steady State

Figure 10. Comparison of Microstructures in Rupture Area

These observations are a further confirmation that internal heating does not radically change the behavior mechanically or metallurgically from that anticipated from isothermal tests. In addition, migration of interstitials up the temperature gradient is either absent or too small to be observed in the limited time of these tests.

One important observation concerning the microstructure of the continuous-heated specimens was the presence of a ferrite layer on the outside surface of the cladding material. This layer can be seen in Figure 10 and is not unexpected since the conditions associated with an internally heated tube favor corrosion and mass transfer.[5] The maximum thickness of the layer occurred in the peak temperature region and was 0.43-mil thick for the 558-hr test. The growth of the ferrite layer for all specimens appears to be parabolic with time, indicating that the growth is diffusion controlled. On the basis that the ferrite layer does not contribute directly to the load-carrying capacity of the tube, it is possible to estimate that the ferrite layer should reduce the stress-rupture life by 4%. This is too small a reduction to be seen in the comparison to the static sodium tests.

On the surface of the internally heated tubes, a polished zone was observed in the region of the heating element. This polished zone is undoubtedly associated with the removal of surface layer by corrosion. However, even for the longest testing time under the steady heat flux, the amount of surface removal was too small to be detected by measurements of the wall thickness. In fact, the extent of surface removal (polishing) was even too small to remove all of the surface scratches introduced in the mill cleaning treatment. Therefore, as in the case for ferrite layer growth, the effect of surface removal was not observable in the stress-rupture behavior of the tubes tested under a steady heat flux. This does not necessarily mean that neither surface removal of metal nor growth of ferrite layers are problems in the prediction of the long term behavior of pressurized tubes with internal heating.

In summary, the stress-rupture behavior of tubes of Type 304 stainless steel under a constant steady internal heat flux of 10^6 Btu/ft^2-hr and with a high internal pressure can be directly predicted from data obtained in static sodium for the stress and temperature corresponding to the peak midwall position of the constant-heated tubes. In addition, the average strain rate of the constant-

heated tubes agreed with that predicted from tests in static sodium. The similarity in microstructures and cracking morphology, coupled with the agreement in stress rupture behavior, indicates that creep-rupture behavior can be accurately predicted directly from stress-rupture tests under internal pressure but without internal heating.

D. STRESS-RUPTURE UNDER CYCLIC HEATING

1. Results

The main goal of the stress-rupture tests in which tubes of Type 304 stainless steel are pressurized and exposed to a cyclic heating is to simulate the variation in heat flux through the wall of the fuel cladding as a result of load variations to the reactor. In the present tests, the internal heater is turned off and on. This is the only difference between these tests and the steady-state tests. Therefore, it is useful to compare the results of these tests with those of the steady heated tests.

The strain profiles obtained for the tests under a cyclic heat flux exhibited some important differences when compared to those under steady heating. The strain at the peak temperature was 50% greater for the cyclic tests than for the steady heating tests. Also, the strain profile was much sharper for the cyclic heat flux condition, indicating that deformation was more localized under this test condition. This comparison is illustrated in Figure 8. It should be pointed out that the profiles for all the cyclic tests were almost identical in size and shape. It is highly likely that the observed plastic deformation occurred during the "heat on" portion of cycle because both the temperature and the stress were larger during this time, a point which is discussed later. What is important here is that operating the internal heater in a cyclic mode brings about an accelerated rate of deformation above that obtained under steady heating. In addition, the strain is localized.

The appearance of the microstructure and the cracking were different for the thermally cycled specimens in contrast to the steady-heated specimens. This can be seen by comparing the microstructures in Figure 10. For the cyclic heat flux condition, the amount of void formation is essentially limited to the region surrounding the failure in the tube. On the other hand, voids were present throughout the cross-section of the steady-heated tubes. This perhaps means

that most of the deformation took place in the region where the cracks were nucleated in the cycled specimens. The absence of extensive void formation, except in the rupture area, indicates that thermal cycling brings into play different deformation mechanisms than for steady conditions or isothermal tests in static sodium.

Cracking under thermal cycling and internal pressurization is intergranular. In this sense, the mechanisms of failure are the same for both kinds of test. However, in three of the tubes tested under a cyclic heat flux, multiple fractures were observed. This suggests that cracking may be autocatalytic in nature, viz. once a crack is nucleated, it propagates independently of any other cracks present. Occasionally, multiple cracks have been seen in the isothermal tests in static sodium. None were observed in the two steady-heated specimens. What is important is that thermal cycling causes clearly observable differences in the peak strain at failure, the strain profile, the extent of void formation, and the number of observable cracks.

The thermally cycled specimens and the steady-heated specimens did show some expected similarities. The failures all occurred at the peak temperature position along the cladding. In the case of multiple ruptures, the cracks were all at the same peak position but at different locations around the tube. The appearance of the microstructures, except for void formation, was the same for both the cyclic and the steady tests. There were:

1) Carbides at the grain boundaries

2) Little or no sigma phase present

3) Slight evidence of recrystallization at the inner surface

4) A thin ferrite layer present on the outside surface. The ferrite layer was thinner for the cyclic specimens than for the steady-heated specimen which ran 500 hours. This is to be expected because, in addition to the internal heating, the time at temperature is important in the growth of the ferrite layer.

It is possible to make a direct comparison between the stress rupture life under cyclic heating and that under steady-state heating. However, the steady-state tests compared directly with the static sodium data. Therefore, because the amount of data for the steady state is limited, it is more fruitful to compare

the cyclic tests with the static sodium tests.

An approach to the analysis of thermally cycled tubes under biaxial tension is that creep rate is a known function of stress and temperature. For a narrow temperature range, we may assume the average creep rate obeys a law of the form:

$$\dot{\bar{\epsilon}} = A\sigma^n \exp\left[kn\, T/100\right] \qquad \ldots(3)$$

where

$\dot{\bar{\epsilon}}$ = average creep rate

A = material constant

n = stress parameter = 3*

kn = temperature parameter = 0.9,* and

T = average temperature (°F).

Since both the temperature and stress vary due to cyclic heater operation, the specimen spends half the time above and below some average stress and temperature. This means that the stress and temperature at the outer surface vary by $\pm\Delta T$ and $\pm\Delta\sigma$. Applying these two extremes to Equation 3 gives,

$$\dot{\bar{\epsilon}} = \dot{\bar{\epsilon}}_0 \left\{\left[1 + \frac{n(n-1)}{2}\left(\frac{\Delta\sigma}{\sigma}\right)^2\right] \cosh \frac{kn\Delta T}{100} + \left[\frac{n\Delta\sigma}{\sigma}\right] \sinh \frac{kn\Delta T}{100}\right\} \qquad \ldots(4)$$

where

$\dot{\bar{\epsilon}}$ = creep rate at the average temperature and stress.[8]

The parameters for this equation were derived from static sodium data. On the basis of the calculated temperature distribution (ΔT = 25°F), and the static sodium stress-rupture (k, n,), the creep rate should increase by 34% over that at the average temperature of 1240°F. On basis of creep in static sodium, the specimen life should be 370 hours at an average stress of 25,000 psi and temperature of 1240°F. In contrast, the tubes ruptured at 200 hours and the actual creep rate was twice that in static sodium. Thus, thermal cycling accelerates the creep rate beyond that anticipated from stress and temperature cycling alone.

*Values derived from static sodium tests.

The comparison between predicted life and observed life is illustrated in Figure 11. This difference between theory and experiment illustrates the danger in indiscriminate use of creep equations to predict the behavior of fuel cladding as the result of reactor load cycles.

Two important test parameters, the frequency and the internal pressure, were varied for the cyclic tests in dynamic sodium. The frequency dependence is important because it is necessary to extrapolate laboratory test conditions to the lower cycle rates expected in fast reactors. The validity of the results of the cyclic tests depends in part on how the frequency of cycling affects the creep behavior. In the case of the present tests, two frequencies were selected. The 12-min cycle was chosen because it gives 1000 cycles in a 200-hr test. In the course of 1000 days, the reactor fuel cladding will experience at least 1000 daily load variations. Thus, the test simulates the number of cycles experienced by fuel cladding. The 2-min cycle was selected to determine the frequency effect, and this frequency could be conveniently achieved with the present test facilities.

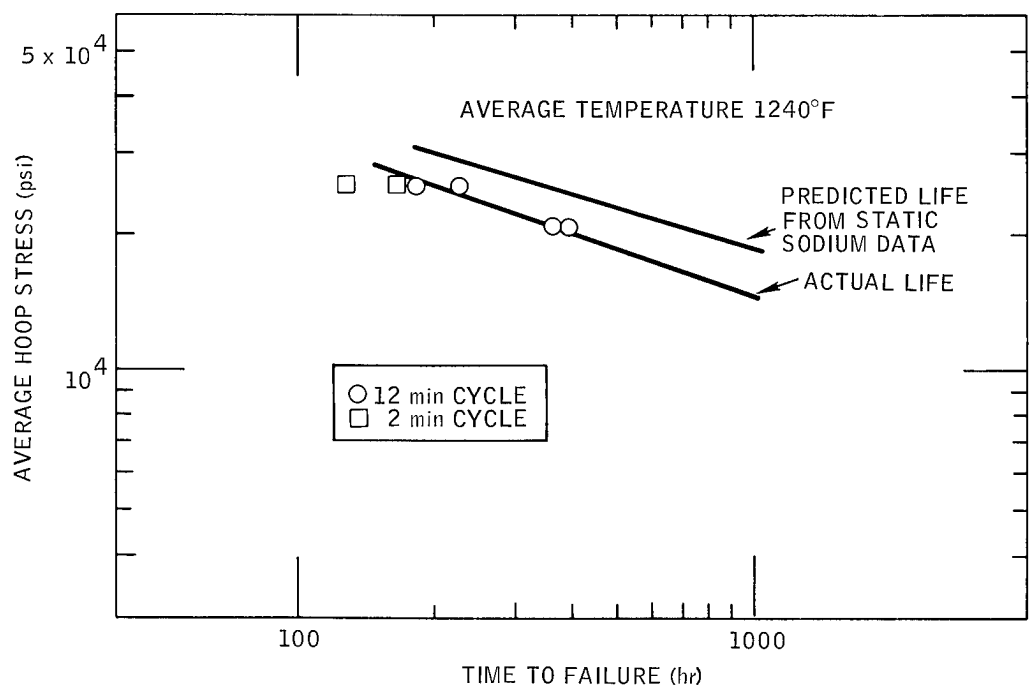

Figure 11. Predicted Life vs Actual Life for 8-A15-063-5A
for Stress Rupture

The increased cycle rate did reduce the life of the specimen by a small amount. However, the life was not decreased by a factor as great as that of the frequency increase. Thus, if there were no cycling frequency effect, the tubes cycled at a higher rate would have had six times the number of cycles. This is not the case, however, as they lasted only 4000 cycles. The lack of a large frequency effect is an important observation since, if thermal fatigue were operative, the frequency would be a large factor in the life of the specimen.[7]

The influence of the mechanical stress on the creep behavior for thermally cycled specimens in flowing sodium is important to the life whether failure is due to thermal fatigue or enhanced creep mechanisms. If creep is operative, then the stress-rupture life should reflect the stress and temperature sensitivity of primary and secondary creep. As shown in Figure 11, the effect of a reduction in the internal pressure (hoop stress) is roughly parallel to the predicted behavior. This parallel slope suggests that creep is primarily responsible for failure and the deformation preceding it.

2. Discussion

The behavior of materials under cyclic stresses superimposed on static stresses has been the subject of several investigations.[9-13] A problem with a direct comparison to these studies is that cyclic stresses superimposed on static stresses can give rise to three basic mechanisms of deformation:

1) Low-cycle fatigue

2) Incremental creep

3) Ratcheting.

The line of distinction is not always clearly made or discernible. Before an analysis of the thermal cycling effects observed in the present work can be made, it is necessary to present at least a qualitative description of the possible mechanisms and what they predict. It should be noted that the fourth alternative mode of deformation is conventional secondary creep. However, this has already been shown to underestimate the thermal cycling effect.

Low-cycle fatigue, including thermal fatigue, has been the object of much interest.[14-16] The principal relation describing low-cycle fatigue is the Coffin equation,[8]

$$e_p N^n = C \qquad \ldots (5)$$

where

e_p = the plastic strain per cycle

N = the number of cycles to failure

n = a material-test parameter = 1/2

C = material-frequency parameter.

In the case of low-cycle fatigue, the plastic strain per cycle is simply the width of the mechanical hysteresis curve. As such, it involves both a tension and a compression region in most cases. It can, however, take place when the mean stress is not zero. Even in this case, the strain range reaches a fixed amount, so that the strain per cycle is not accumulative. In fact, for those cases where tests were conducted with an initial mean stress, the deformation gradually shifted the hysteresis curve downward so that a compressive stress developed during the cycling. The present tests do not appear to conform to what is expected during thermal fatigue. There is a possibility that, once a crack is initiated, it propagates by a fatigue mechanism when the stress or temperature is cycled. However, thermal fatigue cannot rationalize the large peak temperature strains observed for these tests. It is likely that crack nucleation occupies a major portion of the time to rupture. Thus, for the present study on thermal cycling, low-cycle fatigue will not be considered further.

Incremental creep is akin to the strain softening effect frequently seen in low-cycle thermal fatigue. For the case of fatigue, the peak stress of the hysteresis curve decreases to some saturation level. A similar mechanism to this can operate during thermal cycling with internal pressure. Here the main influence of cycling is to reduce the work hardening rate by increasing the rate of recovery in secondary creep. As a result of the decreased work hardening rate, the secondary creep rate is raised. Also, the material is effectively softened. Thus, the rate of deformation and the total amount of strain at failure are increased as a result of thermal cycling.

Incremental creep is clearly a potential mechanism to explain the observed behavior of the cyclic creep specimens, particularly because the material was

used in the 1/8 hard condition, 12-1/2% cold work. Stress activated recovery of the cold work may be accelerated more by cycling. In fact, the behavior of the cold worked tubes in isothermal tests shows that recovery processes are enhanced by stress in such a way that the stress-rupture curve for the cold worked tubes crosses over the annealed curve. Thus, the behavior seen for these tests in which stresses were cycled can be qualitatively explained by a strain softening effect.

The enhancement of creep by a ratchet mechanism is also a possible mechanism by which the present observation on the cycled tubes can be explained. During the "on" portion of the heat cycle, the induced thermal stress relaxes by primary creep. This gives rises to a strain gradient in the wall of the tube. During the "off" portion of the heat cycle, only the mechanical stress due to internal pressure and the residual stresses created by the strain gradient are present. The strain-induced stresses are opposite to the thermal stresses created by internal heating. Thus, during the "off" half cycle, the non-uniform stresses again relax by primary creep. Because of the lower average temperature during the "off" period, the extent of creep is less than during the "on" period. For the present tests, the thermal stress relaxation is almost complete during the "on" period, but may not be complete during the "off" period. As a result, in the next heat cycle, less thermal stress can be generated because the strain is present and reduces this stress. After a few cycles, the extent of creep during each half cycle is such that total strain per cycle is constant.

It should be possible to calculate the amount of damage created per cycle by using the creep equation for primary and secondary creep. This equation is

$$\epsilon_T = \epsilon_0 + \epsilon_t \left(1 - e^{-t/\tau}\right) + \epsilon_s t \qquad \ldots (6)$$

where

ϵ_T = total strain

ϵ_0 = initial strain on loading

ϵ_t = limiting transient creep strain

τ = ratio of transient creep rate to transient creep strain

t = time

ϵ_s = secondary or minimum creep rate[16]

There are some data available from the literature for describing creep in annealed 18-8 stainless steel at 704°C.[17] Since the peak stresses relax during both the "on" and "off" half cycles, the application of the data to the present situation is complicated because the parameters in Equation 6 are sensitive to stress. In addition, the temperature of the present work is lower for both half cycles. Nevertheless, the data can be used to estimate the value of the creep strain during each half cycle. To estimate the creep strain per cycle, it is necessary to pass through a transient period before a saturation effect in cycling is reached. The transient and saturation behaviors are depicted in Figure 12.

At the beginning of the first half cycle, a thermal stress in the wall is established by the heat flux by differential thermal expansion. The strain gradient and the associated thermal stress decrease during the heat-on part of the cycle due to primary creep. This decrease is evident in the stress and strain profiles at the end of the first half cycle. At the start of the second half cycle, the heat

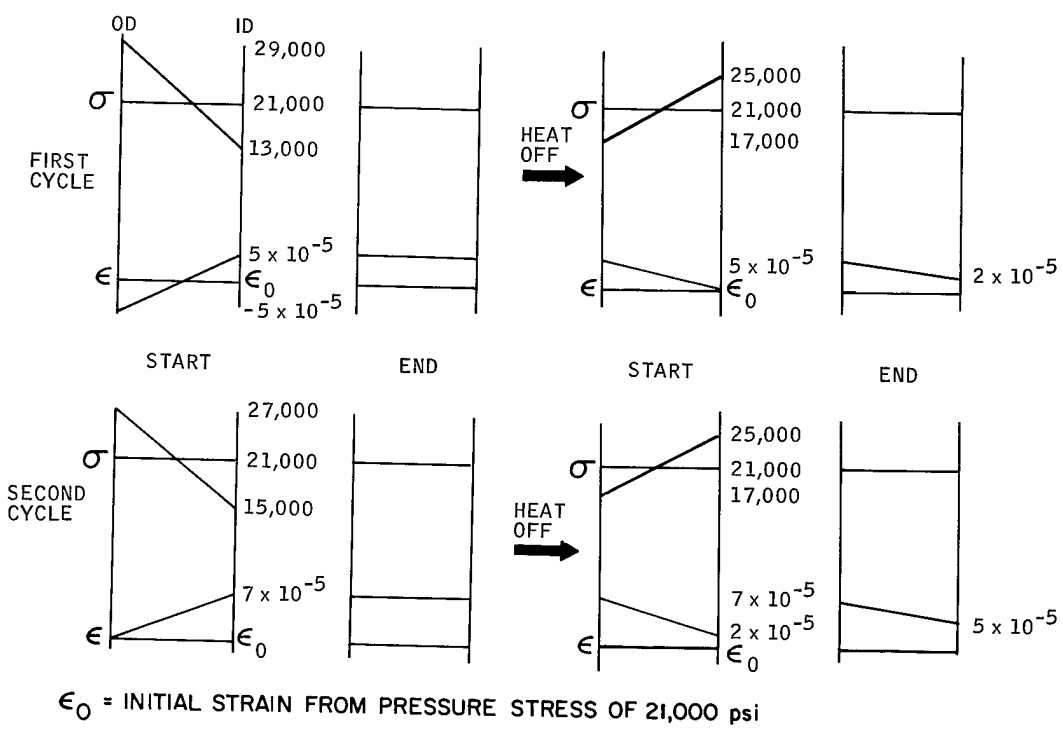

Figure 12. Effect of Thermal Cycling on Stress and Strain Profiles

flux is removed and the thermal gradient becomes zero. The strain distribution, however, is non-uniform. Thus, at the start of the second half cycle the strain gradient gives rise to a residual stress gradient opposite to the thermal stress gradient. Under the combined action of the residual stress and the pressure stress, the material creeps. This creep is non-uniform and partly removes the residual stress. This is because at the lower temperature primary creep during the heat off half cycle is less than that which took place during the previous half cycle. The situation at the end of the second half cycle shown in Figure 12 reflects the partial stress relaxation.

During subsequent cycles, primary creep is altered. At the start of the third half cycle, the heat flux induces a strain gradient which is partly cancelled by the already existing strain gradient of opposite sign. The net effect produces a smaller strain gradient from internal heating than existed during the first half cycle and consequently a smaller thermal stress. This thermal stress relaxes completely by the end of the third half cycle. As before, when the heat flux is turned off, the non-uniform plastic strain creates reverse residual stress. As before, this residual stress partly relaxes by the end of the fourth half cycle. Additional cycles repeat the situation for the second cycle approaching a minimum amount of creep deformation per cycle. The minimum amount of primary creep is determined by that creep which takes place during the second half of each cycle.

The process of ratcheting will go on until the cladding fails under the internal gas pressure and thermal cycling. Adding the creep strains developed during the off period of each cycle gives a total creep deformation of 3% for 1000 cycles. While this estimate is lower than the actual deformation of 3.6%, a low estimate can easily be attributed to a neglect of secondary creep and to the initial plastic strain after internal pressurization.

The mechanism described above can be extended to qualitatively explain the effects of frequency of cycling on the stress-rupture life of the internally heated specimens. In review, when the frequency was increased by a factor of 6, the strain per cycle decreased by a factor of 4. This simply reflects the influence of primary creep which is an exponential function of time. At the higher cycle rate, the period of time during which creep takes place is 1/6 that

of the earlier tests. Since primary creep is non-linear in time, proportionally more creep can occur during the 1-min half cycle than during the 6-min half cycle. This means that in one minute the amount of creep strain is more than 1/6 ($\leq$ 1/4) that for a 6-min half cycle. (In fact, using the same creep data, it appears that the creep strain per cycle for the higher frequency is indeed one fourth.) If all the creep strain were due to secondary creep, which is linear in time, the higher cycle rate should result in one-sixth the creep strain per cycle and six times the number of cycles than for the slower cycle rate. This is not observed. In this work, the specimens experienced only 4000 cycles at the higher rate and one-fourth the strain per cycle. Thus it appears that, while secondary creep may occur, most of the deformation is associated with primary creep during each cycle.

The influence of the mean pressure stress on creep-rupture under cyclic heating can also be explained using the creep equations described previously. The tests at lower mechanical pressure stress, but at the same internal heat flux and cycle rate, showed a longer stress-rupture life. This is undoubtedly a direct result of a smaller amount of primary creep during the off portion of the cycle. The decreased strain then limits the amount of creep due to increased thermal stress during the next period. The creep rupture life under cyclic behavior paralleled that for the steady-heated specimens. The parallel behavior is perhaps a manifestation of the stress dependency of creep. Both secondary creep and primary creep are reported to have the same functional relation to stress.[17]

The British have treated the thermal cyclic effect in detail.[9,10] While many of the ideas presented above are essentially the same as those presented by the British, one important difference must be considered. In the British work, the increased strain resulting from cycling the internal heat flux takes place because of the non-linear dependence of secondary creep on the stress. This is undoubtedly valid for the case where the specimens are cycled every 100 hours. However, the results for thermal cycling do not conform to use of secondary creep in the analysis as was indicated earlier. Moreover, it is not possible to rationalize the frequency effect observed in this study by a secondary creep mechanism or incremental creep mechanism. However, secondary creep is likely to play an important role for longer cycle periods such as 24 hr. Nevertheless, for all cycle rates, primary creep should be considered in addition to secondary creep in describing the ratcheting mechanism of deformation.

IV. CONCLUSIONS

The results of tests with internally heated and pressurized cladding in flowing sodium clearly showed the versatility and value of a high flux heater assembly in simulating the non-nuclear aspects of a fuel pin environment. While the device is still in the development stage, it has already provided considerable insight into the phenomena associated with stress-rupture, corrosion, and ratcheting under conditions which approximate those found in fast reactors. Major findings are described below with the engineering implications of the results.

The experiments showed that pressurization with NaK instead of helium (as in static sodium tests) did not have an observable effect on stress-rupture properties. Neither did the flowing sodium cause an effect on stress-rupture properties with respect to those obtained in static sodium or helium environments. In the case of the control and the internally heated specimens, mass transfer was observed, but the extent was too small to affect stress-rupture life.

The results of the tests with internally heated and pressurized specimens operated in a cyclic mode show a pronounced influence on the stress-rupture life and the rate of deformation. The differences in the strain at failure, grain boundary void formation, and strain profiles indicate that thermal cycling alters creep deformation mechanisms over a considerable portion of the life of the specimen. It was found that conventional secondary creep equations cannot rationalize the increased strain or the reduction in life. However, when primary creep is superimposed on each cycle, both the observed frequency effect and the influence of the mechanical stress can be explained using a ratcheting mechanism. While the quantitative agreement is perhaps fortuitous, analysis of the results shows that primary creep must be considered (in addition to secondary creep) in the analysis of behavior under internal heating and pressure when the heat flux is cycled.

These results from initial experiments have several significant implications to design and selection criteria for fuel cladding. The abbreviated life, the increased strain at rupture, and the modified deformation mode under a cyclic thermal heat flux suggest that a ratcheting mechanism can operate. While the

thermal cycling tests were short-term relative to the desired life of fuel cladding, analysis of the experimental results indicates that both primary and secondary creep must be included in the design considerations. In application, the thermal stresses generated by the heat flux will be nearly twice as great because of the greater cladding wall thickness. The reactor load variations reduce the temperature of the fuel to remove part of the steady tangential load on cladding; but the fission gas pressure, coupled with the thermal stresses, can still cause the proposed mechanism to operate. During the time the fuel imposes load on the cladding, the situation is aggravated by an additional cyclic load.

Another implication to design is that static NaK or sodium do not reduce the rupture life of fuel cladding. This is particularly important to the sodium bonded fuels where the liquid metal provides a thermal bond to the cladding.

The tests with control specimens revealed that wires can interact with the cladding. These kinds of interactions, while too small to affect the short-term life of the cladding, may eventually become important to wire wrap spacer concepts. This is particularly true if the wires are rigid and become bound between fuel pins due to swelling.

The results of microstructural observations on the internally heated specimens indicated the presence of a ferrite layer. This layer was too small to reduce the life of cladding. For times greater than 3000 hours, the parabolic growth rate of the layer found for these specimens is great enough to expect a 20% reduction in life. Using the conservative assumption that the ferrite layer contributes nothing to the strength of the alloy, corrosion allowances based on only surface layer removal are not optimistic, even when the thickness of the ferrite layer reaches an equilibrium thickness.

The design of LMFBR will require additional work in the areas outlined above. Nevertheless, these initial experiments have contributed to a better rationale for describing the effects of the non-nuclear aspects of cladding service, and they have provided groundwork for future developmental investigations. Additional information is needed about the effects of alloy type, alloy state, thermal stress, and mass transfer on creep rupture under both continuous and cyclic heat fluxes.

REFERENCES

1. W. T. Lee, "Biaxial Stress-Rupture Properties of Austenitic Stainless Steels in Static Sodium," AI-AEC-12694 (to be published)
2. E. W. Murbach, J. E. Bodine, and N. W. Heath, "The Systems-Quality Sodium Loop," NAA-SR-12327 (May 31, 1967)
3. R. L. McKisson and E. L. Babbe, "High Flux Heater Design and Development," AI-AEC-12681 (to be published)
4. ASTM Standards, Part 31, p 453 (May 1967)
5. J. Hopenfeld and D. K. Darley, "Dynamic Mass Transfer of Stainless Steel in Sodium Under High-Heat-Flux Conditions," NAA-SR-12447 (July 15, 1967)
6. "Sodium Components Development Program, Mass Transfer Investigation in Liquid Metal Systems, Quarterly Progress Report No. 2, June - August 1967," GEAP-5546
7. H. Susskind, "Behavior of Fuel Cladding Under Load and With Thermal Cycling in Sodium," BNL 50010 (1966)
8. L. F. Coffin, Jr., "The Problem of Thermal Stress Fatigue in Austenitic Steels at Elevated Temperatures," Symposium on Effect of Cyclic Heating and Stressing of Metals, ASTM STP No. 165, Philadelphia (1954)
9. J. Bree, "Ratchet and Fatigue Mechanism in Sealed Fuel Pins for Nuclear Reactors," TRG Rep 1214(D) (March 1966)
10. J. Bree, "Ratchet and Enhanced Creep Strains in Sealed Fuel Pins for Nuclear Reactors," TRG Rep 1311(D) (August 1966)
11. G. J. Moyar and G. M. Sinclair, "Cyclic Strain Accumulation Under Complex Multiaxial Loading," Paper 35, International Conference on Creep, Inst. Mech. Eng., London, p 2 (47) (1963)
12. A. H. Melaka, "Combined Fatigue and Creep," Met. Rev. 7 43 (1962)
13. S. Tarra and M. Ohnami, "Fracture and Deformation of Metals Subjected to Thermal Cycling Combined with Mechanical Stress," Paper 25, International Conference on Creep, Inst. Mech. Eng., London, p 3-57 (1963)
14. E. Glenny, "Thermal Fatigue," Metallurgical Reviews 6 (1961)
15. L. F. Coffin and R. P. Wesley, Trans ASME 76 923 (1954)
16. G. R. Halford and S. S. Manson, "Application of a Method of Estimating High Temperature Low Cycle Fatigue Behavior of Materials," NASA-TMX-52357 (October 19, 1967)
17. F. Garofalo, "Fundamentals of Creep and Creep-Rupture in Metals," Macmillan, New York, p 10-27 (1966)